Color-neutral superconducting quark matter

Andrew W. Steiner

Department of Physics and Astronomy, State University of Stony Brook, Stony Brook, New York 11794

Sanjay Reddy

Center for Theoretical Physics, Massachusetts Institute of Technology, Cambridge, Massachusetts 02139

Madappa Prakash

Department of Physics and Astronomy, State University of Stony Brook, Stony Brook, New York 11794

We investigate the consequences of enforcing local color neutrality on the color superconducting phases of quark matter by utilizing the Nambu–Jona-Lasinio model supplemented by diquark and the 't Hooft six-fermion interactions. In neutrino free matter at zero temperature, color neutrality guarantees that the number densities of u, d, and s quarks in the color-flavor-locked (CFL) phase will be equal even with physical current quark masses. Electric charge neutrality follows as a consequence and without the presence of electrons. In contrast, electric charge neutrality in the less symmetric 2-flavor superconducting (2SC) phase with ud pairing requires more electrons than the normal quark phase. The free energy density cost of enforcing color and electric charge neutrality in the CFL phase is lower than that in the 2SC phase, which favors the formation of the CFL phase. With increasing temperature and neutrino content, an unlocking transition occurs from the CFL phase to the 2SC phase with the order of the transition depending on the temperature, the quark and lepton number chemical potentials. The astrophysical implications of this rich structure in the phase diagram, including estimates of the effects from Goldstone bosons in the CFL phase, are discussed.

Studies of QCD at high baryon density have led to the expectation that quark matter is a color superconductor in which the pairing gaps of unlike quarks (ud, us, and ds) are as large as 100 MeV. For three massless flavors, a symmetric ground state called the color-flavor-locked (CFL) phase, in which BCS-like pairing involves all nine quarks, is favored [1,2]. At lower density and for physically relevant values of the strange current quark mass ($100 < m_s / \text{MeV} < 300$), a less symmetric [2-flavor superconducting (2SC)] phase in which only the light up and down quarks ($m_{u,d} \lesssim 10$ MeV) pair is expected [3,4]. For recent reviews, see Refs. [5].

With the exception of the work by Iida and Baym [6], and more recently by Alford and Rajagopal [7], little attention has been paid to the issue of color neutrality in superconducting quark phases. These works are the primary motivation for this study. The issues addressed in this work are similar to those addressed by Alford and Rajagopal [7] who perform a model independent analysis that is valid when $m_s \ll \mu$ and $\Delta \sim m_s^2/\mu$, where Δ is the pairing gap and μ is the quark number chemical potential. We employ an extended version of the the Nambu–Jona-Lasinio (NJL) model, which shares many symmetries with QCD, including the spontaneous breaking of chiral symmetry, and calculate the thermodynamic potentials, Ω, and pairing gaps, Δ, self-consistently in the CFL and 2SC phases. Our analysis leads to results that complement some of the conclusions in Ref. [7]. There are, however, several aspects in which we go further. First, we employ a self-consistent model which uniquely determines both the diquark and the quark-antiquark condensates. Second, since the realization of color and electric charge neutrality becomes non-trivial only for physically relevant values of m_s, we retain terms to all or-

ders in m_s in our calculation of Ω. As noted in Ref. [7], this is particularly important for understanding the phase structure of quark matter at densities (or equivalently, μ) of relevance to neutron stars, since m_s/μ is not small compared to unity. In addition, we establish the phase structure of superconducting color-neutral quark matter at finite temperature and lepton content which was not considered in [6,7], but is relevant for studies of proto-neutron stars.

Charges, chemical potentials, and color neutrality. Bulk, homogeneous matter must be neutral with respect to charges which interact through the exchange of massless gauge bosons. Otherwise, the free energy density cost would be infinite. In the CFL phase, diquark condensation breaks color symmetry and all eight gluons become massive via the Higgs mechanism. Similarly, in the 2SC phase, $SU(3)_c$ is broken down to $SU(2)_c$ and five of the eight gluons become massive. In both the CFL and 2SC phases, however, a $U(1)$ gauge symmetry remains unbroken [1]. The associated charge is called $\tilde{Q}$. The generator for this charge in the CFL phase is a linear combination of the usual electric charge Q and a combination of color generators T_3 and T_8, and is given by

$$\tilde{Q} = Q - \frac{1}{2}T_3 - \frac{1}{2\sqrt{3}}T_8, \qquad (1)$$

where $Q = \text{diag}(2/3, -1/3, -1/3)$ in flavor space, and $T_3 = \text{diag}(1, -1, 0)$ and $T_8 = \text{diag}(1/\sqrt{3}, 1/\sqrt{3}, -2/\sqrt{3})$ in color space.

The color superconducting phase is, by construction, neutral with respect to $\tilde{Q}$ charge. Why then should we impose, in

addition, local color neutrality? As noted earlier, gluons become massive in the superconducting phase and the free energy density cost of realizing a non-zero color density in bulk matter need not be infinite. Further, although a finite sample embedded in the normal state must be a color singlet, this alone does not require local color neutrality since color singletness is a global constraint. Hence a heterogeneous phase with colored domains of typical size similar to the color Debye screening length is a possibility. However, in a homogeneous and color conducting medium a color charge density in the bulk is unstable as it generates a chromo-electric field resulting in the flow of color charges [7]. Color neutrality is therefore a requirement for the homogeneous phase. Neutrality with respect to charges associated with T_3 and T_8 is achieved by introducing appropriate chemical potentials μ_3 and μ_8 in analogy with the charge chemical potential μ_Q. As noted in Refs. [7,8], color neutrality is a prerequisite for color singletness, but the additional free energy density cost involved in projecting out the color singlet state is negligible for large samples.

The superconducting ground state breaks both color and electromagnetic gauge symmetries. It would therefore seem that excitations above the condensate can only be characterized by the unbroken $\tilde{Q}$ charge. At first sight, this would imply that electrons and unpaired quarks carry only $\tilde{Q}$ charge and must therefore be assigned only a $\mu_{\tilde{Q}}$ chemical potential. If this were indeed the case, it would be impossible to neutralize the 2SC phase in the bulk. This is because the condensate is $\tilde{Q}$ neutral, but has color and electric charge that cannot be neutralized by particles with only $\tilde{Q}$ charge. The resolution to this puzzle lies in noting that our expectation to assign only those charges that are unbroken by condensation to excitations applies only to excitations above a charge-neutral ground state. In this case, charges associated with broken gauge symmetries are easily delocalized and transported to the surface by the condensate. It is, however, important to note that only the excess broken charge resides on the surface. In describing particles that make up the charge neutral ground state we must use vacuum quantum numbers. In this case, the individual charges are localized on the particles in the bulk. Therefore, in what follows we treat electrons and unpaired quarks as carrying their vacuum charges in our description of the neutral ground state.

Thermodynamics. We begin with the NJL Lagrangian [9–14] supplemented by both a diquark interaction and the 't Hooft six-fermion interaction which reproduces the anomalous $U_A(1)$ symmetry breaking present in QCD [15]. Explicitly,

$$
\mathcal{L} = \bar{q}_{i\alpha}(i\partial\!\!\!/\,\delta_{ij}\delta_{\alpha\beta} - m_{ij}\delta_{\alpha\beta} - \mu_{ij,\alpha\beta}\gamma^0)q_{j\beta}
$$

$$
+ G_S\sum_{a=0}^{8}[(\bar{q}\lambda_f^a q)^2 + (\bar{q}i\gamma_5\lambda_f^a q)^2] - G_D[\det_{ij}\bar{q}_{i\alpha}
$$

$$
\times(1+i\gamma_5)q_{j\beta} + \det_{ij}\bar{q}_{i\alpha}(1-i\gamma_5)q_{j\beta}]\delta_{\alpha\beta}
$$

$$
+ G_{DIQ}\sum_{k}\sum_{\gamma}[(\bar{q}_{i\alpha}\epsilon_{ijk}\epsilon_{\alpha\beta\gamma}q_{j\beta}^C)
$$

$$
\times(\bar{q}_{i'\alpha'}^C\epsilon_{i'j'k}\epsilon_{\alpha'\beta'\gamma}q_{j'\beta'}) + (\bar{q}_{i\alpha}i\gamma_5\epsilon_{ijk}\epsilon_{\alpha\beta\gamma}q_{j\beta}^C)
$$

$$
\times(\bar{q}_{i'\alpha'}^C i\gamma_5\epsilon_{i'j'k}\epsilon_{\alpha'\beta'\gamma}q_{j'\beta'})], \tag{2}
$$

where m_{ij} is the diagonal current quark matrix, and the spinor $q^C = C\bar{q}^T$, where C is the Dirac charge conjugation matrix. We use α, β, γ for color (r=red, b=blue, and g=green) indices, and i,j,k for flavor (u=up, d=down, and s=strange) indices throughout. The chemical potential matrix is diagonal in flavor and color, and is given by

$$
\mu_{ij,\alpha\beta} = (\mu\delta_{ij} + Q_{ij}\mu_Q)\delta_{\alpha\beta} + \delta_{ij}(T_{3\alpha\beta}\mu_3 + T_{8\alpha\beta}\mu_8), \tag{3}
$$

where μ is the quark number chemical potential. Since the couplings G_S, G_D, and G_{DIQ} are dimensionful, we impose an ultraviolet three-momentum cutoff, Λ, and results are considered meaningful only if the quark Fermi momenta are well below this cutoff. The values of the couplings are fixed by reproducing the experimental vacuum values of f_π, m_π, m_K, and $m_{\eta'}$ as in Ref. [10]. For the most part, we discuss results obtained using

$$
m_{0u} = m_{0d} = 5 \text{ MeV}, \quad m_{0s} = 140 \text{ MeV},
$$

$$
\Lambda = 600 \text{ MeV}, \quad G_S\Lambda^2 = 1.84, \tag{4}
$$

$$
G_D\Lambda^5 = 12.4, \quad \text{and} \quad G_{DIQ} = 3G_S/4.
$$

In vacuum, the effective four-fermion interactions in the qq and $\bar{q}q$ channels are related by a Fierz transformation, hence the choice of $G_{DIQ} = 3G_S/4$. Note that Eq. (2) does not include the possible presence of a six-fermion interaction due to diquark ($\langle qq\rangle$) condensates; such interactions have been assumed to result only in a renormalization of the four-fermion diquark interaction. In the mean field approximation, the thermodynamic potential per unit volume is given by

$$
\Omega = -2G_S\sum_{i=u,d,s}\langle\bar{q}_i q_i\rangle^2 + 4G_D\langle\bar{u}u\rangle\langle\bar{d}d\rangle\langle\bar{s}s\rangle
$$

$$
-\sum_{k}\sum_{\gamma}\frac{|\Delta^{k\gamma}|^2}{4G_{DIQ}} - \frac{1}{2}\int\frac{d^3p}{(2\pi)^3}
$$

$$
\times\sum_{i=1}^{72}\left[\frac{\lambda_i}{2} + T\ln(1+e^{-\lambda_i/T})\right] + \Omega_0, \tag{5}
$$

where $\langle\bar{q}_i q_i\rangle(i=u,d,s)$ is the quark condensate, and the term Ω_0 ensures that the zero density pressure, $P = -\Omega$, of non-superconducting matter is zero:

$$
\Omega_0 = 2G_S\sum_{i=u,d,s}\langle\bar{q}_i q_i\rangle_0^2 - 4G_D\langle\bar{u}u\rangle_0\langle\bar{d}d\rangle_0\langle\bar{s}s\rangle_0
$$

$$
+ 2N_c\sum_{i}\int\frac{d^3p}{(2\pi)^3}\sqrt{m_i^2 + p^2}, \tag{6}
$$

where $\langle \overline{q}_i q_i \rangle_0$ denotes the value of the quark condensate at zero density. The gap matrix

$$\Delta^{k\gamma} = 2G_{DIQ} \langle \overline{q}_{i\alpha} i \gamma_5 \varepsilon^{ijk} \varepsilon^{\alpha\beta\gamma} q_{j\beta}^C \rangle \qquad (7)$$

features three non-vanishing elements. Using the standard notation of denoting $\Delta^{k\gamma}$ through the flavor indices i and j, we have

$$\Delta_{ds} \equiv \Delta^{ur}, \quad \Delta_{us} \equiv \Delta^{dg}, \quad \text{and} \quad \Delta_{ud} \equiv \Delta^{sb}. \qquad (8)$$

This corresponds to the ansatz in Ref. [2], except that color sextet gaps (symmetric in both color and flavor) are ignored. Inclusion of the sextet gaps modifies our results only slightly, because such gaps are small [2]. Note, however, that we have removed the degeneracy between Δ_{us} and Δ_{ds} in order to explore phases in which these gaps may not be equal.

The quasiparticle energies λ_i may be obtained by diagonalizing the inverse propagator. Equivalently, λ_i are the eigenvalues of the (72×72) matrix

$$D = \begin{bmatrix} -\gamma^0 \vec{\gamma} \cdot \vec{p} - M_i \gamma^0 + \mu_{i\alpha} & \Delta i \gamma^0 \gamma_5 C \\ \gamma^0 C i \gamma_5 \Delta & -\gamma^0 \vec{\gamma}^T \cdot \vec{p} + M_i \gamma^0 - \mu_{i\alpha} \end{bmatrix},$$

where M_i are the dynamically generated quark masses and Δ is given by

$$\Delta = \Delta_{ud} \varepsilon^{3ij} \varepsilon^{3\alpha\beta} + \Delta_{us} \varepsilon^{2ij} \varepsilon^{2\alpha\beta} + \Delta_{ds} \varepsilon^{1ij} \varepsilon^{1\alpha\beta}. \qquad (9)$$

Equations (2) through (9) enable a consistent model calculation of the thermodynamics of superconducting quark matter as a function of the chemical potentials μ, μ_Q, μ_3, and μ_8 at arbitrary temperatures. For a given set of these chemical potentials, the dynamical (or constituent-like) masses M_i and the gaps Δ_{ij} are determined by the solutions of equations that result from extremizing Ω with respect to $\langle \overline{q}_i q_i \rangle$ and Δ_{ij}, respectively.

The phases are labeled according to which of the three gaps are non-zero: (1) Normal phase: all gaps zero; (2) 2SC phase: only Δ_{ud} is non-zero; and (3) CFL phase: all gaps are non-zero. Where needed, we add electrons simply by noting that $\mu_e = -\mu_Q$, and include their free Fermi gas contribution to Ω.

Recall that the ground state is $\tilde{Q}$ neutral, i.e., $n_{\tilde{Q}} = -\partial\Omega/\partial\mu_{\tilde{Q}} = 0$, which is a consequence of the fact that the condensates are $\tilde{Q}$ neutral. Quasiparticles carrying $\tilde{Q}$ charge are massive with $m \sim \Delta$. In addition, the $\tilde{Q}$ susceptibility $\chi_{\tilde{Q}} = \partial n_{\tilde{Q}}/\partial\mu_{\tilde{Q}} \simeq 0$; in fact, the free energy density is independent of $\mu_{\tilde{Q}}$ at zero temperature. This is because to generate $\tilde{Q}$ charge in the ground state, we must break a pair and the energy cost is of $O[\Delta]$. In contrast, the free energy density depends on μ_Q, μ_3, and μ_8, and, the corresponding individual susceptibilities do not vanish. For a physical m_s of order 100 MeV, there is no *a priori* reason to expect equal numbers of u, d, and s quarks in the CFL phase. The pairing ansatz in Eq. (8) and the arguments of Rajagopal and Wilczek [16], however, guarantee that
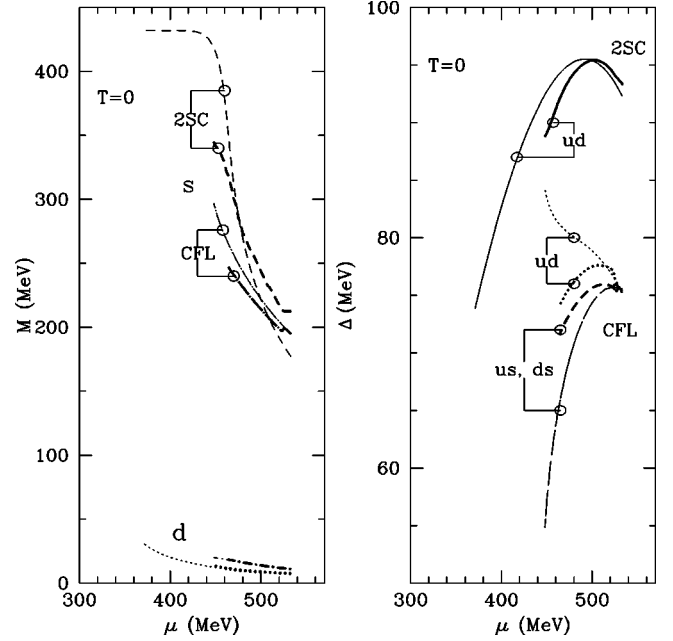
FIG. 1. Dynamically generated masses and pairing gaps in the CFL and 2SC phases at zero temperature from NJL model calculations. Dark (light) curves refer to results when color and electric charge neutrality is (is not) imposed.

$$n_{rd} = n_{gu}, \quad n_{bd} = n_{gs}, \quad \text{and} \quad n_{rs} = n_{bu}, \qquad (10)$$

or equivalently, that

$$n_u = n_r, \quad n_d = n_g, \quad \text{and} \quad n_s = n_b, \qquad (11)$$

where $n_{\alpha i}$ is the number density of quarks with color α and flavor i, and $n_\alpha (n_i)$ is the net number density of color α (flavor i). Pairing by itself does not enforce either color or electric charge neutrality. The strange quark mass induces both color and electric charge in the CFL phase. We are, however, at liberty to adjust the chemical potentials μ_3 and μ_8 to enforce color neutrality. Moreover, since the pairing ansatz enforces $\tilde{Q}$ neutrality, enforcing color neutrality automatically enforces electric charge neutrality at $\mu_Q = 0$. In contrast, the 2SC phase requires a finite μ_Q to satisfy electric charge neutrality and hence admits electrons.

We turn now to discuss results, beginning with those at temperature $T = 0$. In Fig. 1, we show the dynamically generated or constituent d and s quark masses M_i (left panel) and the pairing gaps Δ_{ij} (right panel) as functions of μ in the CFL and 2SC phases. The u quark mass, which tracks the trend of the d quark, is not shown for the sake of clarity. The dark (light) curves refer to the case in which color and electric charge neutrality is (is not) imposed. All masses decrease with increasing μ, since all of the $\langle \overline{q}q \rangle$ condensates decrease with μ. Note that the requirement of color and charge neutrality has a larger effect on the s quark mass in the 2SC phase than in the CFL phase. This is because neutrality in the 2SC phase requires a large and negative electric charge chemical potential. In the discussion that follows, we will show that $\mu_Q \sim -m_s^2/2\mu$ in the 2SC phase. Further, since
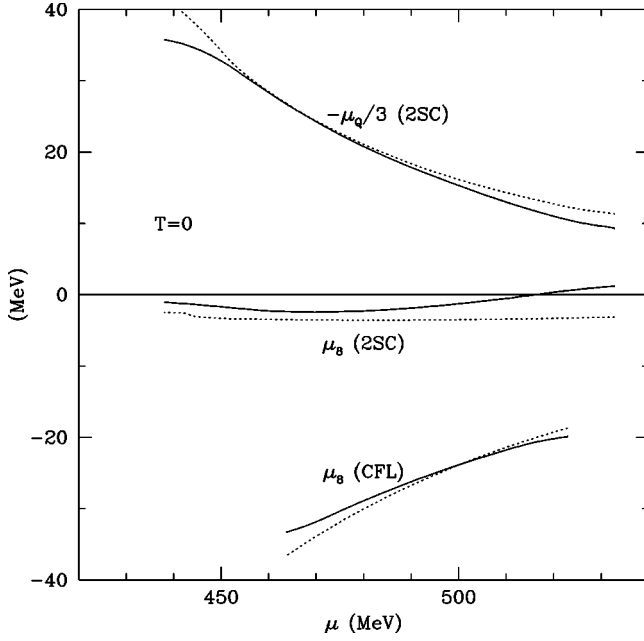
FIG. 2. Chemical potentials μ_8 and μ_Q that ensure color and electric charge neutrality in the CFL and 2SC phases as functions of the quark number chemical potential μ at temperature $T=0$. Solid (dashed) curves refer to results of the NJL (simplified) model.

$\mu_s = \mu - \mu_Q/3$, a large and negative μ_Q enhances the strange quark density which in turn suppresses the $\langle \bar{s}s \rangle$ condensate.

The right panel of Fig. 1 shows the various gaps in the CFL and 2SC phases. Imposing color neutrality reduces Δ_{ud}, since the numbers of red and green quarks (equivalently of u and d quarks) are reduced relative to the colored case (see the analytical analysis below). For the same reason, color neutrality increases the gaps involving strange quarks. These trends are broken only when μ begins to approach the ultraviolet cutoff Λ. The strong increase of the Δ_{ud} gap as μ decreases for matter in which neutrality is not imposed is due to the strong decrease in the gaps involving strange quarks.

In Fig. 2 we show the chemical potentials μ_8 and μ_Q (as functions of μ) required to achieve color and electric charge neutrality in the CFL and 2SC phases. The solid curves refer to results of the NJL model calculations. The left panel of Fig. 3 shows the pressure P versus μ at $T=0$. Here the dark (light) curves refer to the case in which color and electric charge neutrality is (is not) imposed. Note that the pressure of the color and electrically neutral normal phase falls below that of the 2SC phase for all μs shown. The pressure differences ΔP or the free energy density cost necessary to ensure color and electric charge neutrality in the CFL and 2SC phases are shown in the right panel of Fig. 3. Here also the solid curves refer to results of the NJL model calculations.

In order to gain a qualitative understanding of the results in Figs. 2 and 3, we undertake an analytical analysis of a simpler model also considered in Ref. [7]. In this analysis, we consider u and d quarks as massless, and include corrections due to the s quark mass m_s at leading order as a shift in its chemical potential. This does not properly account for the shift in energy due the strange quark mass for states far away from the Fermi surface, but is a consistent approximation in
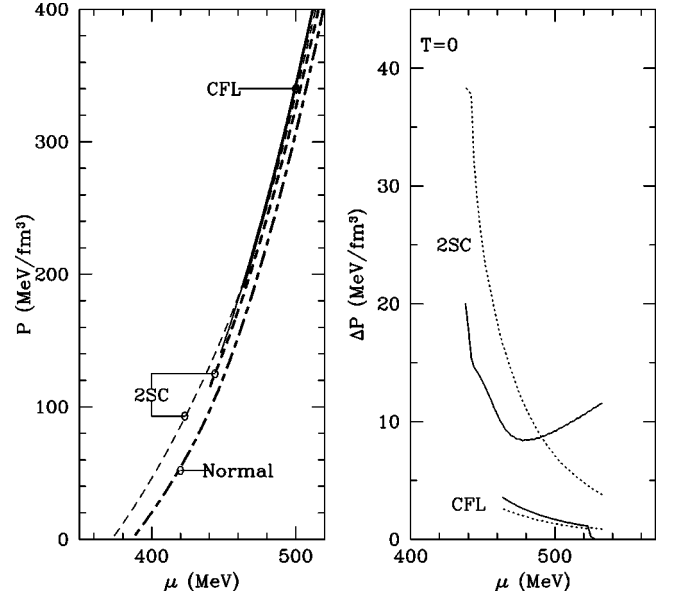
FIG. 3. Left panel: The pressure P versus quark number chemical potential μ in the CFL, 2SC, and normal phases at temperature $T=0$. Dark (light) curves refer to the case in which color and electric charge neutrality is (is not) imposed. Right panel: Pressure differences ΔP or the free energy density cost required to ensure color and electric charge neutrality in the CFL and 2SC phases at $T=0$. Solid (dotted) curves are results of the NJL (simplified) model calculations.

this context since we are primarily interested in the leading order cost of enforcing neutrality. Further, we assume that all gaps, including those involving the s quark, are independent of m_s,[1] and that both the gaps and m_s are weak functions of the chemical potentials. With these assumptions, and to leading order in Δ

$$\Omega_{\text{CFL}} = \Omega_{\text{rgb}} + \Omega_{\text{rg}} + \Omega_{\text{rs}} + \Omega_{\text{gs}},$$

$$\Omega_{\text{rgb}} = -\frac{1}{12\pi^2}[\mu_1^4 + \mu_2^4 + \mu_3^4 + 3\Delta^2(\mu_1^2 + \mu_2^2 + 4\mu_3^2)],$$

$$\Omega_{\text{rg}} = -\frac{1}{6\pi^2}(\mu_{\text{rg}}^4 + 3\Delta^2\mu_{\text{rg}}^2), \qquad (12)$$

$$\Omega_{\text{rb}} = -\frac{1}{6\pi^2}(\mu_{\text{rb}}^4 + 3\Delta^2\mu_{\text{rb}}^2),$$

$$\Omega_{\text{gb}} = -\frac{1}{6\pi^2}(\mu_{\text{gb}}^4 + 3\Delta^2\mu_{\text{gb}}^2),$$

where we have written the free energy of the CFL phase in terms of the 3×3 block involving $ru - gd - bs$ quarks, and three 2×2 blocks involving $rd - gu$, $rs - bu$ and $gs - bd$

---

[1]Corrections to Δ due to m_s arise at $O[m_s^2/\mu]$; for a detailed discussion, see Ref. [17].

quarks, respectively. Each of the three 2×2 blocks is rigid in the sense that the free energy is unaffected by differences in chemical potentials of quarks that pair in a given block [16]. The free energy depends only on the average chemical potential. The 3×3 block does not exhibit this rigidity; here, the quasi-particle energies depend on the splitting between the chemical potential characterizing the ru, gd, and bs quarks. Chemical potentials that characterize the free energy of the 3×3 block are given by

$$\mu_1 = \mu + \frac{\mu_8}{\sqrt{3}}, \quad \mu_2 = \mu - \frac{\mu_8}{\sqrt{3}} - \frac{m_s^2}{3\mu},$$

$$\mu_3 = \mu - \frac{m_s^2}{6\mu}, \quad (13)$$

and the common chemical potentials that appear in the free energy expressions of the 2×2 blocks are given by

$$\mu_{rg} = \mu + \frac{\mu_8}{\sqrt{3}}, \quad \mu_{rb} = \mu - \frac{\mu_8}{2\sqrt{3}} - \frac{m_s^2}{4\mu},$$

$$\mu_{gb} = \mu - \frac{\mu_8}{2\sqrt{3}} - \frac{m_s^2}{4\mu}. \quad (14)$$

We note that, in general, pairing between particles with dissimilar masses does not require a common chemical potential. Maximal BCS-like pairing requires that the distribution of the pairing partners be identical in momentum space. Since we treat the u and d quarks as massless particles and account for the effects of the s quark mass through a shift in the chemical potential in our analytic analysis, a common chemical potential within each pairing block ensures that the aforementioned pairing criterion is satisfied.

In the CFL phase, the stress induced by the strange quark mass generates color charges. In the limit of nearly equal and vanishing light quark masses, the CFL scheme in Eq. (11) indicates that we will require only a non-zero μ_8 to achieve color neutrality. This justifies why we neglect μ_Q and μ_3 in Eqs. (13) and (14). To leading order in the parameter m_s^2/μ, and assuming that the differences between the various gaps are small and μ, m_s independent, we find that

$$\mu_8(\text{CFL}) = -\frac{1}{2\sqrt{3}} \frac{m_s^2}{\mu} + O\left[\frac{m_s^4}{\mu^3}, \frac{m_s^2 \Delta^2}{\mu^3}\right] \quad (15)$$

by requiring $\partial \Omega_{CFL}/\partial \mu_8 = 0$. Since $n_u = n_d$ and hence $n_r = n_g$ when there are no electrons, $\mu_3(\text{CFL}) = 0$ identically in the CFL phase at zero temperature. Naively, Eq. (15) would imply that the free energy density cost of enforcing color neutrality in the CFL phase is of $O[m_s^2 \mu^2]$. However, we find that such contributions are absent due to cancellations. This result (see the lower-most dotted curve in Fig. 2), with m_s and Δ of the NJL model as inputs, provides an excellent

approximation to the exact NJL result. Utilizing Eq. (15), we find an analytic estimate for the free energy density cost in the CFL phase:

$$\Delta \Omega_{CFL} = \Omega_{CFL}(\mu_8) - \Omega_{CFL}(0) = \frac{5m_s^4}{72\pi^2} + O\left[\frac{m^6}{\mu^2}, \frac{m^4 \Delta^2}{\mu^2}\right]. \quad (16)$$

The lower dotted curve in the right panel of Fig. 3 shows that this result is in quantitative agreement with the NJL model calculation.

In the 2SC phase, the pairing phenomenon itself gives rise to color charges. The 2SC thermodynamic potential, to leading order in the gap and consistent with the approximation scheme described earlier, is

$$\Omega_{2SC} = \Omega_{rugd} + \Omega_{free},$$

$$\Omega_{rugd} = -\frac{1}{3\pi^2}(\mu_{rugd}^4 + 3\Delta^2 \mu_{rugd}^2), \quad (17)$$

$$\Omega_{free} = -\frac{1}{12\pi^2}(\mu_{bu}^4 + \mu_{bd}^4 + \mu_{bs}^4 + \mu_{rs}^4 + \mu_{gs}^4 + \mu_Q^4).$$

The chemical potentials appearing above are defined by

$$\mu_{rugd} = \mu + \frac{\mu_8}{\sqrt{3}} + \frac{\mu_Q}{6}, \quad \mu_{bu} = \mu - \frac{2\mu_8}{\sqrt{3}} + \frac{2\mu_Q}{3},$$

$$\mu_{bd} = \mu - \frac{2\mu_8}{\sqrt{3}} - \frac{\mu_Q}{3}, \quad \mu_{bs} = \mu - \frac{2\mu_8}{\sqrt{3}} - \frac{\mu_Q}{3} - \frac{m_s^2}{2\mu}, \quad (18)$$

$$\mu_{rs} = \mu_{gs} = \mu + \frac{\mu_8}{\sqrt{3}} - \frac{\mu_Q}{3} - \frac{m_s^2}{2\mu}.$$

The condition to ensure color neutrality, $\partial \Omega_{2SC}/\partial \mu_8 = 0$, yields

$$\mu_8(\text{2SC}) = -\frac{1}{3\sqrt{3}} \frac{\Delta^2}{\mu} + O\left[\frac{\Delta^4}{\mu^3}\right], \quad (19)$$

where we have used a common value of Δ (independent of μ) in the analytical analysis. Note that $\mu_8(\text{2SC})$ does not depend on m_s at leading order. Since pairing in the 2SC phase involves red and green quarks, it does not induce a color 3-charge; hence $\mu_3(\text{2SC}) = 0$. However, electric charge neutrality in the 2SC phase requires an adjustment due to the magnitude of m_s. At leading order in a $1/\mu$ expansion, we find

$$\mu_Q(\text{2SC}) = -\frac{1}{2} \frac{m_s^2}{\mu} - \frac{1}{3} \frac{\Delta^2}{\mu} + O\left[\frac{m_s^4}{\mu^3}, \frac{\Delta^2 m_s^2}{\mu^3}\right] \quad (20)$$

by setting $\partial\Omega_{2SC}/\partial\mu_Q=0$. As in the CFL phase, the free energy density cost of enforcing color neutrality in the 2SC phase is small, because $O[\Delta^2\mu^2]$ terms cancel and the free energy density begins to change at $O[\Delta^4]$. Similarly, we find that there is no cost for enforcing electric charge neutrality in the 2SC phase at $O[\mu^2]$. Using the results in Eqs. (19) and (20), the free energy density cost of enforcing color and electric charge neutrality becomes

$$\Delta\Omega_{2SC}=\Omega_{2SC}(\mu_8,\mu_Q)-\Omega_{2SC}(0,0)$$

$$=\frac{1}{8\pi^2}\left(m_s^4+\frac{4\Delta^2 m_s^2}{3}+\frac{4\Delta^4}{3}\right)$$

$$+O\left[\frac{m_s^6}{\mu^2},\frac{\Delta^6}{\mu^2},\frac{\Delta^2 m_s^4}{\mu^2}\right]. \quad (21)$$

Although the free energy density costs of enforcing color neutrality in the CFL and 2SC phases are of the same order, the cost in the 2SC phase is numerically larger. This is in part due to the larger strange quark mass in the 2SC phase and because the free energy density cost due to Δ- and m_s-dependent terms add in the 2SC phase. The analytical results in Eqs. (19), (20), and (21), shown as dotted curves in Figs. 2 and 3, compare well with the results of the NJL model.

Phase diagram at finite temperature and lepton content. In the proto-neutron star context, matter is subject to stresses induced by finite temperature and lepton number chemical potentials [18]. Since electrons have both electric and lepton number charges,

$$\mu_e=-\mu_Q+\mu_{Le}, \quad (22)$$

where $\mu_{Le}=\mu_{\nu_e}$ is the chemical potential for electron lepton number. In order to explore the effects of a finite neutrino chemical potential and finite temperature on the superconducting phases, we employ the NJL model, Eq. (5) with extensions to include neutrinos and electrons.

Figure 4 shows representative cross-sectional views of the $T-\mu-\mu_{\nu_e}$ phase diagram. The left panel displays results at fixed $\mu=460$ MeV. With increasing temperature, a first order transition occurs from the CFL phase to the 2SC phase with ud pairing. For $\mu_{Le}=0$, the transition occurs at $T\simeq17$ MeV. The corresponding baryon densities are $n_B=(n_u+n_d+n_s)/3=1.06$ fm^{-3} in the CFL phase and $n_B=0.94$ fm^{-3} in the 2SC phase. At zero neutrino chemical potential, an analytic estimate of the critical temperature T_c for the CFL-2SC transition can be obtained by assuming that the gaps in the 2SC and CFL phases are nearly equal to each other and to their zero temperature values. We find that

$$T_c=\frac{\sqrt{2}}{\pi}\Delta_0\left[1-\frac{4}{5}\frac{\delta\Delta}{\Delta_0}\xi_{BCS}^2+\frac{9}{20}\frac{m_s^2}{\Delta_0^2}\frac{\delta m_s}{m_s}\right]\xi_{BCS}$$

with $\xi_{BCS}=\left(1+2\frac{\Delta_0^2}{\pi^2 T_{BCS}^2}\right)^{-1}$, $\quad (23)$
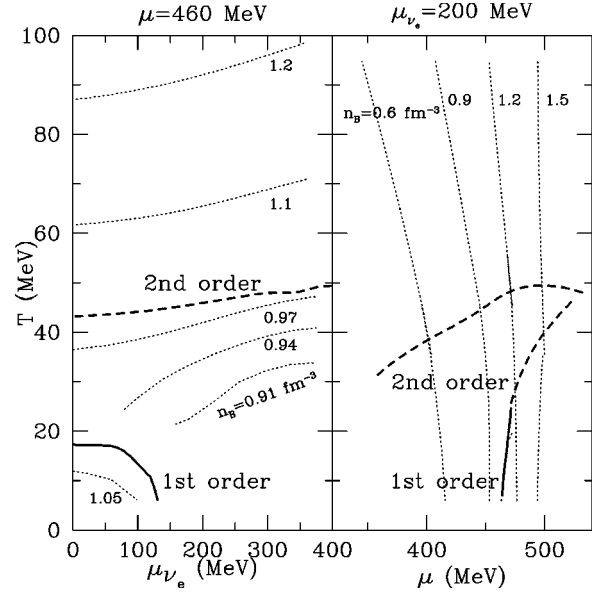
FIG. 4. Cross-sectional views of the $T-\mu-\mu_{\nu_e}$ phase diagram at the indicated values of μ and μ_{ν_e}. In both panels, the dark curves show the phase boundaries, while the dotted curves show contours of constant baryon density.

where Δ_0 is the zero temperature gap, $\delta\Delta$ and δm_s are the differences between the gaps and the strange quark masses in the 2SC and CFL phases, respectively. T_{BCS} is the temperature at which the gap in the CFL phase would vanish, assuming that $\Delta(T)=\Delta_0\sqrt{1-(T/T_{BCS})^2}$. Note that, in general, gaps involving strange quarks do not vanish at the transition, i.e., the phase transition is first order. This is because at leading order, the critical temperature $T_c\sim\Delta_0/2.22$ is less than that for the second order BCS transition, $T_{BCS}\simeq\Delta_0/1.76$. It is clear from Eq. (23) that contributions to T_c due to $\delta\Delta$ and δm_s can easily alter this, allowing for a BCS like second order transition. If the magnitude of the gap in the 2SC phase is larger than that in the CFL phase, T_c is lowered and the transition becomes more strongly first order.

Accommodating a finite lepton number in the CFL phase is expensive, because the requirement of color and electric charge neutrality in this phase excludes electrons. At $T=0$, the transition from the CFL to 2SC phase occurs at $\mu_{Le}\simeq150$ MeV. The latent heat density, $T\Delta(\partial P/\partial T)$, lies in the range $(2-15)$ MeV/fm^3 along the boundary of the first order phase transition. With increasing temperature, the critical lepton chemical potential at which the CFL-2SC transition occurs decreases. This is because the gaps in the CFL phase decrease with increasing T; consequently, unlocking occurs at smaller μ_{ν_e}.

The right panel in Fig. 4 shows the phase boundaries at fixed $\mu_{\nu_e}=200$ MeV. For this neutrino chemical potential, the CFL phase is preferred above $\mu=460$ MeV. For low (high) values of μ, the region of the CFL phase shrinks (expands) progressively to lower (higher) values of T and μ_{ν_e}. In contrast, the 2SC-normal phase boundary is relatively unaffected by increasing values of μ (in the range relevant for proto-neutron star studies), although minor

variations do occur. Note that with increasing temperature, the phase transition switches from first to second order. This switch is due to the fact that the Δ_{us} and Δ_{ds} gaps decrease along the first order phase transition line. When these gaps vanish (at $T \sim 25$ MeV for $\mu_{\nu_e} = 200$ MeV), the phase transition becomes second order. In Fig. 4, contours of constant baryon density are shown by the dotted curves in both panels. Notice that, for the values of μ and μ_{ν_e} chosen for display, the 2SC phase supports lower baryon densities than the CFL phase. Across the first order phase transition, the density contours are discontinuous. We wish to add that the phase in which $\Delta_{us} \neq \Delta_{ds}$ was found to be thermodynamically disfavored in the range of T, μ, and μ_{ν_e} explored here.

The consequences of requiring local color neutrality in superconducting quark matter with and without neutrinos at both zero and finite temperatures are the principal findings of this work. Quantitative results, especially those for quark number chemical potentials approaching the ultraviolet cutoff in the NJL model used, should be viewed with some caution. Notwithstanding this, the basic qualitative features concerning the phase transitions appear to be generic, insofar as similar trends are found in our analytic analysis that employed a simplified model without a cutoff. We also wish to emphasize that the phase diagram in Fig. 4 requires revision at low values of μ (or low baryon densities) for which a hadronic phase is more likely to be favored.

Kaon condensation. In neutrino-free matter, Bedaque and Schafer have shown that the strange quark mass induces a stress which can result in the condensation of neutral kaons in the superconducting quark phase [19,20]. Kaon condensation occurs when the stress induced by the strange quark mass $m_s^2/(2\mu) \gtrsim m_{K^0}$, where m_{K^0} is the mass of the neutral kaon. In general, the masses of all pseudo Goldstone bosons receive contributions both from the diquark and quark-antiquark condensates. For example, the mass of the neutral kaon is given by [21–24]

$$m_{K^0}^2 = a m_u (m_d + m_s) + \chi (m_d + m_s), \qquad (24)$$

where $a \sim \Delta^2/\mu^2$ and $\chi \sim \langle \bar{q}q \rangle$. At asymptotically high density, where the axial $U(1)$ symmetry is restored and the quark-antiquark condensate vanishes, the dominant contribution to the masses is from the diquark condensate. In this case, the kaon masses become small, of order 10 MeV, and kaon condensation is robust. At the densities of relevance to neutron stars, the situation is less clear because a finite $\langle \bar{q}q \rangle$ can potentially result in larger masses for the kaons and disfavor meson condensation [22,24]. Pending a detailed investigation of this question within the NJL model, we assess here how kaon condensation can affect the structure of the color-neutral phase by assuming that the kaon mass is small compared to $m_s^2/(2\mu)$. This corresponds to near maximal kaon condensation. In this case, the meson contribution to the pressure is easily computed and is given by [20]

$$P_{K^0} = \frac{1}{2} f_\pi^2 \left[\frac{m_s^2}{2\mu} \right]^2 \left(1 + O\left[\frac{m_{K^0}^2 \mu^2}{m_s^4} \right] \right), \qquad (25)$$

where $f_\pi \sim \mu$ is the pion decay constant in the effective theory describing Goldstone bosons [21]. The leading contribution to the pressure from the Goldstone bosons is of order m_s^4. Including this contribution we find that at zero temperature and neutrino chemical potential, the phase transition between the 2SC and CFLK0 phases occurs at a value of μ which is lower by 16 MeV compared to the case without kaons.

At finite neutrino chemical potential, CFL quark matter contains a K^+ condensate which admits electrons, even at zero temperature [20]. In the presence of electrons, charged kaon condensation lowers the free energy density cost for accommodating lepton number. Including the electron and K^+ contributions to the pressure ($P_{K^+} = f_\pi^2 \mu_{K^+}^2/2$), and solving self-consistently for the condition of charge neutrality, the pressure is increased by about 2 MeV at $\mu_{\nu_e} = 200$ MeV. These results indicate that the extent of the meson condensed CFL phase in the phase diagram is likely to be enlarged, but only by a few percent. In our analysis, the order of the phase transitions between the CFL and the 2SC phase was not affected by meson condensation. We wish to note, however, that our analysis neglects the effect of the meson condensate on the quasi-particles themselves. This feedback, which can alter the quark contribution to the free energy, must be explored before quantitative conclusions regarding the role of meson condensation on the phase diagram can be drawn. This warrants further investigation and is beyond the scope of this article.

Astrophysical implications. The $T - \mu - \mu_{\nu_e}$ phase diagram offers clues about the possible phases encountered by a neutron star from its birth as a proto-neutron star (in which neutrinos are trapped) in the wake of a supernova explosion to its neutrino-poor catalyzed state with ages ranging from hundreds of thousands to million years. In earlier work, some aspects of how a phase transition from the normal to the 2SC phase would influence neutrino transport in a newly born neutron star were explored [25]. To date, detailed calculations of the evolution of a proto-neutron star with quarks have been performed for the case in which only the normal phase was considered [26]. Our findings in this work indicate that the core of a proto-neutron star may well encounter a 2SC phase first when matter is hot and neutrino-rich before passing over to a CFL phase.

Conclusions. Color and electric charge neutrality in the superconducting quark phases requires the introduction of chemical potentials for color and electric charge. The magnitudes of these chemical potentials are subleading in μ. The corresponding free energy density costs are small and independent of μ at leading order with the free energy density cost for neutrality in the 2SC phase being significantly larger than that in the CFL phase. Consequently, and in agreement with Ref. [7], we find that the bulk 2SC phase is less likely to occur in compact stars at $T=0$ and $\mu_{\nu_e}=0$. In the NJL model, a small 2SC window does exist at relatively low baryon density. However, since this window occurs at very low density it is likely to be shut by the hadronic phase. If homogeneous quark matter were to occur in neutron stars, it

seems likely that with increasing μ a sharp interface would separate hadronic matter and CFL quark matter [27]. We note, however, that we have only considered homogeneous phases in this study and it is possible that less symmetric heterogeneous phases may well be favored for chemical potentials of relevance to neutron stars. Examples include the CFL-hadron mixed phase [27] and crystalline superconductivity [28]. These possibilities alleviate the cost of enforcing color neutrality, since in these cases it is only a global constraint. In such phases, however, energy costs associated with gradients in particle densities must be met.

The value of the diquark coupling employed in this work predicts gaps on the order of 100 MeV at $\mu \simeq 500$ MeV. The relationship between the $\langle qq \rangle$ and $\langle \bar{q}q \rangle$ condensates in medium obtained by employing the mean-field gap equations with the couplings set by the Fierz transformation in vacuum may differ from that obtained in a more exact treatment of the NJL model. Lacking experimental guidance on their values in medium, we have studied the influence of moderate changes to the diquark coupling (but within the mean-field approximation) on the predicted phase structure. For example, using $G_{DIQ} = G_S$, we find that gaps are increased by about 20% in both the CFL and 2SC phases relative to the case with $G_{DIQ} = 3G_S/4$ predicted by the Fierz transformation in vacuum. The extent of the low density region in which a 2SC phase is favored over the CFL phase is not greatly changed and the 2SC phase continues to be favored over the normal phase.

Had we ignored the differences in the strange quark mass between the charge-neutral normal phase and the charge-neutral 2SC phase, the normal phase would be favored over the 2SC phase at low density when $\Delta \lesssim m_s^2/4\mu$ [7]. However, we find that the chemical potential for the strange quarks is larger in the charge-neutral 2SC phase than that in the normal phase. Consequently, $\langle \bar{s}s \rangle$ is reduced and the lighter strange quarks in the 2SC phase contribute more to the pressure. It is this feedback that tips the balance in favor of the 2SC phase when $\Delta \lesssim m_s^2/4\mu$. However, we do not expect this trend to remain intact for larger variations in the couplings. Obviously, it is always possible to reduce G_{DIQ} and increase G_S so as to allow for the existence of a normal phase at lower density. At finite temperature and neutrino chemical potential, the CFL phase becomes less favored both because of its small specific heat and because of its exponentially suppressed [by the factor $\exp(-\Delta/T)$] electron number density, which makes the free energy density cost of accommodating lepton number large. In contrast, the 2SC phase has a larger specific heat and easily accommodates electron number, and is therefore the favored phase at finite temperature and lepton number.

The inclusion of Goldstone bosons in the CFL phase tends to extend the region in the T-μ_{ν_e} plane where the CFL phase is favored, since Goldstone bosons contribute significantly to the specific heat and also allow for the presence of electrons. In the absence of Goldstone bosons, a first order unlocking transition occurs from the CFL phase to the less symmetric 2SC phase with increasing lepton chemical potential. When the temperature is sufficiently high, the phase transition switches from first to second order due to the fact that the Δ_{us} and Δ_{ds} gaps decrease along the first order phase transition line and eventually vanish.

As discussed above, different phases of color superconducting quark matter are likely to be traversed by the inner core of a proto-neutron star during its early thermal evolution. The task ahead is to study how these phases and transitions between them influence observable aspects of core collapse supernova, neutron star structure, and thermal evolution.

---

[1] M. Alford, K. Rajagopal, and F. Wilczek, Nucl. Phys. **B537**, 443 (1999).

[2] M. Alford, J. Berges, and K. Rajagopal, Nucl. Phys. **B558**, 219 (1999).

[3] M. Alford, K. Rajagopal, and F. Wilczek, Phys. Lett. B **422**, 247 (1998).

[4] R. Rapp, T. Schäfer, E.V. Shuryak, and M. Velkovsky, Phys. Rev. Lett. **81**, 53 (1998).

[5] R. Rapp, T. Schäfer, E.V. Shuryak, and M. Velkovsky, Ann. Phys. (N.Y.) **280**, 35 (2000); K. Rajagopal and F. Wilczek, in *At the Frontier of Particle Physics/Handbook of QCD*, edited by M. Shifman (World Scientific, Singapore, 2001), Vol. 2, Chap. 35; M. Alford, Annu. Rev. Nucl. Part. Sci. **51**, 131 (2001).

[6] K. Iida and G. Baym, Phys. Rev. D **63**, 074018 (2001).

[7] M. Alford and K. Rajagopal, J. High Energy Phys. **06**, 031 (2002).

[8] P. Amore, M.C. Birse, J.A. McGovern, and N.R. Walet, Phys. Rev. D **65**, 074005 (2002).

[9] Y. Nambu and G. Jona-Lasinio, Phys. Rev. **122**, 345 (1961).

[10] P. Rehberg, S.P. Klevansky, and J. Hüfner, Phys. Rev. C **53**, 410 (1996).

[11] M. Buballa and M. Oertel, Phys. Lett. B **457**, 261 (1999).

[12] A.W. Steiner, M. Prakash, and J.M. Lattimer, Phys. Lett. B **486**, 239 (2000).

[13] M. Buballa and M. Oertel, Nucl. Phys. **A703**, 770 (2002); M. Oertel and M. Buballa, hep-ph/0202098.

[14] R. Nebauer and J. Aichelin, Phys. Rev. C **65**, 045204 (2002).

[15] G. 't Hooft, Phys. Rep. **142**, 357 (1986).

[16] K. Rajagopal and F. Wilczek, Phys. Rev. Lett. **86**, 3492 (2001).

[17] J. Kundu and K. Rajagopal, Phys. Rev. D **65**, 094022 (2002).

[18] M. Prakash, I. Bombaci, Manju Prakash, P.J. Ellis, J.M. Lattimer, and R. Knorren, Phys. Rep. **280**, 1 (1997).

[19] P.F. Bedaque and T. Schäfer, Nucl. Phys. **A697**, 802 (2002).

[20] D.B. Kaplan and S. Reddy, Phys. Rev. D **65**, 054042 (2002).

[21] D.T. Son and M.A. Stephanov, Phys. Rev. D **61**, 074012 (2000); **62**, 059902 (2000).

[22] C. Manuel and M.H. Tytgat, Phys. Lett. B **479**, 190 (2000).

[23] T. Schäfer, Phys. Rev. D **65**, 074006 (2002).

[24] T. Schäfer, Phys. Rev. D **65**, 094033 (2002).

[25] G.W. Carter and S. Reddy, Phys. Rev. D **62**, 103002 (2000).

[26] J.A. Pons, A.W. Steiner, M. Prakash, and J.M. Lattimer, Phys. Rev. Lett. **86**, 5223 (2001).

[27] M.G. Alford, K. Rajagopal, S. Reddy, and F. Wilczek, Phys. Rev. D **64**, 074017 (2001).

[28] J.A. Bowers and K. Rajagopal, Phys. Rev. D **66**, 065002 (2002).